

Evolution of the Globular Cluster System in a Triaxial Galaxy

R. Capuzzo–Dolcetta,¹ A. Tesserì,¹

¹ *Istituto Astronomico, Università La Sapienza,*

Via G. M. Lancisi 29, I-00161, Roma, Italy

dolcetta@astrmb.rm.astro.it, tesseri@astrmb.rm.astro.it

Accepted yr m d. Received yr m d; in original form yr m d

ABSTRACT

Dynamical friction and tidal disruption are effective mechanisms of evolution of globular cluster systems, especially in non-axisymmetric galaxies with a central compact nucleus. With a semi-analytical approach based on the knowledge of the dependence of the dynamical friction and tidal disruption effects on the relevant parameters, we are able to follow the time evolution of the globular cluster system in a model of a triaxial galaxy and give its observable properties to compare with observational data.

An important result is that the flatter distribution of the globular cluster system relatively to that of the stellar bulge, as observed in many galaxies, can be explained by the evolution of the globular cluster system, starting from the same density profile.

Key words: galaxies: star clusters – galaxies: kinematics and dynamics

1 INTRODUCTION

Two observational facts are well established, by now:

i) the first is that many galaxies have globular clusters systems (GCSs) with density profiles less concentrated than their parent galaxy halo light, M87 and M49 being the prototypes (Lauer & Kormendy 1986, Harris 1986, 1991). This has been recently confirmed by observations of a sample of 14 elliptical galaxies, made with the WFPC2 of the Hubble Space Telescope (Forbes et al. 1996). These observations, thanks to the high resolution of the HST, were able to probe the inner kiloparsecs of those galaxies and show that most, if not all, of them have GCSs with surface density profiles that rise towards the centre less steeply than the underlying galaxy light;

ii) the second is that many galaxies host compact massive nuclei in their centres (Dressler & Richstone 1988, Kormendy 1988, Kormendy & Richstone 1995, Eckart & Genzel 1996) with estimated masses in the range from $2 \cdot 10^6 M_\odot$ for our Galaxy and M32 up to $3 \cdot 10^9 M_\odot$ for M87.

An explanation for the difference between halo star and globular cluster distributions has been proposed by Harris & Racine (1979), Harris (1986), and Racine (1991) as a difference in the formation epoch of the two components. In this scenario, the GCS formed in an earlier phase of the protogalactic collapse, while the stars that constitute the halo condensed later, this resulting in a less peaked distribution for the clusters. This picture requires an exact timing in the sequence of the evolution, in order to permit the clusters to be less metal rich than the halo stars, while pro-

ducing the required differences in central concentration. In disk galaxies, however, 'the epoch of cluster formation would be early enough to force chemical enrichment but not early enough to take on a distinct spatial structure' (Harris 1986, Sect. VII, p. 840). Moreover, this scenario does not explain why the tails of the two density distributions are almost the same. This last observational evidence suggests an alternative explanation: the cluster system and the halo formed at the same time with a similar spatial distribution, and the present differences are a consequence of the dynamical evolution of the GCS. Dynamical evolution correlates also with the possible presence of massive central nuclei. Actually, the larger core radius of the GCS would imply that the globular cluster population has been significantly depauperated in the inner regions of the system. This is the case when a massive object (like a black hole) resides in the centre of a galaxy and disrupts, by means of tidal forces, globular clusters which pass sufficiently close to it. There is no direct evidence that the aforementioned massive objects are black holes (they could be, as proposed by Kormendy & Richstone (1995), massive clusters of low-mass stars, stellar remnants etc.) except in the case of NGC 4258, where the discovery of a perfect keplerian rotation curve in the inner regions (Miyoshi et al. 1995) rules out, on dynamical evidences (Mayoz 1995), alternatives to black holes. In the outer regions, on the contrary, the influence of the central massive object will be negligible. So we expect that there the cluster distribution has remained more or less unchanged.

Another major dynamical effect, the dynamical friction of field stars on globular clusters, enhances the efficiency of

the depleting mechanism. It acts reducing the cluster orbital energy and bringing the clusters towards the centre, thus increasing the number of globular clusters in the inner regions. These clusters could feed the massive object. This scenario has been proposed first by Tremaine, Ostriker and Spitzer (1975), in a study on M31, where they showed how a massive object of mass in the range 10^7 – $10^8 M_\odot$ could directly form from globular clusters braked to the centre of the galaxy and there merged.

Both of these effects (dynamical friction and tidal disruption) are significantly emphasized if the galaxy is triaxial in shape, a possibility supported by several observations (see, for example, Bertola, Vietri & Zeilinger (1991) which show evidence of triaxial distributions in 32 galaxies). The orbits which constitute the bulk of such a potential are the ‘box’ orbits, which are dense around the centre (see, e. g., Binney & Tremaine 1987, hereafter BT) where the massive object lies (so that even globular clusters of large apocentric distance will possibly be disrupted) and the field star density is higher (so that dynamical friction efficiency is increased). In fact, Pesce, Capuzzo Dolcetta and Vietri (1992) have demonstrated that dynamical friction decay times on box orbits are significantly reduced.

The shape of the velocity ellipsoid of halo stars and globular clusters in our galaxy supports this picture. In fact, while the velocity dispersion of the halo stars is larger in the radial direction, as expected from numerical simulation of the radial collapse of the protogalaxy, the globular clusters’ velocity ellipsoid is almost spherical. Under the hypothesis of a coeval formation, this can be explained by a selective process which destroyed the clusters on low-angular momentum orbits (i.e. box orbits in a triaxial galaxy). The role of triaxiality in the tidal disruption mechanism has been quantitatively discussed by Ostriker, Binney and Saha (1989) (hereafter OBS). In their paper they proposed, for the first time, that the formation of a massive nucleus from decayed globular clusters could be a self-limiting process, due to the inverse proportionality of the tidal disruption timescale, τ_{tid} , to the nucleus mass. Capuzzo Dolcetta (1993) has investigated thoroughly the evolution of a GCS in the Schwarzschild’s (1979) triaxial non-rotating model, under the combined effects of dynamical friction and tidal disruption, studying the growth of the nucleus and the evolution of globular clusters’ mass function. Indeed, he found that the cooperation of these two effects may lead to the formation of a compact nucleus, in form of globular clusters decayed to the centre of the galaxy. The growth of the nucleus eventually halts when its mass is large enough to shatter all incoming clusters. Of course the value of the mass reached by the growing nucleus depends, in this scheme, on the initial GCS spatial, mass and velocity distributions.

The increased efficiency of dynamical friction and tidal disruption, in a triaxial galaxy, is so increased that their effects are not limited to the very inner regions of the parent galaxy. Moreover, there is no need to assume, for the GCS, a box-biased phase-space density such that the globular clusters are all on box orbits. In fact, Capuzzo Dolcetta (1993) showed that even in the case of an isotropic distribution function (hereafter DF), the evolution of the GCS is very similar to that of a box-biased DF. The reason for this is that the two DFs do not differ much in the region of the phase-space occupied by the majority of the clusters.

In Section 2 we describe our model of a globular cluster system evolving due to dynamical friction and tidal disruption effects and we give a formula which permits to calculate the density profile of the GCS and its observable properties; in Section 3 we present and discuss the results.

2 THE MODEL

In this paper we study a population of clusters exclusively on box orbits. This may be the case if they formed in the early galactic stages, during the radial collapse of the protogalactic nebula (van Albada 1982, Binney 1988). We develop a semi-analytical model which allows to follow the evolution of the spatial density of the GCS in a triaxial galaxy under the influence of the two main evolutionary effects: dynamical friction and tidal disruption. Once the spatial density profile of the GCS is obtained, we can deduce its surface density profile, core radius and other useful quantities which may be compared to observations. The galactic potential adopted here, like in Pesce et al. (1992) and Capuzzo-Dolcetta (1993), is that of the Schwarzschild’s (1979) model. We define (following Capuzzo Dolcetta 1993) $\tau_{df}(E, m)$ as the time required to a cluster on a box orbit to lose all its energy E (and stop at the centre of the galaxy) by means of the frictional drag exerted by the stellar population. A good fit to $\tau_{df}(E, m)$ is:

$$\tau_{df}(E, m) = \frac{1}{m} \frac{7.5 \cdot 10^8}{(1-E)^2} yr, \quad (1)$$

where m is the mass of the cluster in units of $10^6 M_\odot$ and E ($0 \leq E < 1$) is the orbital energy per unit mass in units of Φ_0 , the central value of the Schwarzschild potential. Equation (1) is not well behaved at the origin since, as the energy approaches zero, $\tau_{df}(E, m)$ reaches a finit limit, which is inconsistent with its definition. In practical calculations we used a slightly different form of Eq. (1), which exhibits the behavior required.

To include the effect of tidal disruption we will need an estimate of the timescale, τ_{tid} , associated to this effect which, according to OBS and Capuzzo Dolcetta (1993), may be expressed in the form

$$\tau_{tid} = \frac{1}{\mu \pi \sqrt{5}} \sqrt{\frac{Gm}{R_h}} \frac{v_n}{v_c^2} \frac{A_w}{r_c R_h} T_r \quad (2)$$

where: $\mu = \frac{GM_n}{r_c v_c^2}$; M_n is the mass of the nucleus; r_c is the core radius of the galaxy; v_c is the circular speed at large r ; v_n is the speed of the cluster of mass m at the point where the gravitational attraction of the ellipsoid equals that of the nucleus; A_w is the area of the waist of the box orbit; R_h is the half-mass radius of the cluster; T_r is the half-period of oscillation parallel to the potential long axis. Note that Eq. (2) depends on the structural parameters of the clusters only through the quantity $\sqrt{\frac{m}{R_h^3}}$ which is proportional to the square root of the mean density within the half-mass radius, $\sqrt{\bar{\rho}_h}$. The dependence of τ_{tid} on the orbital energy E is through A_w , v_n and T_r .

Since we are interested in the density profiles of the GCS, it is useful to treat it as a ‘fluid’ system. This allows us to adopt the continuity equation as the one which rules the evolution of the system:

$$\frac{\partial \rho}{\partial t} + \frac{\partial \rho v_r}{\partial r} + 2 \frac{\rho v_r}{r} = -S \quad (3)$$

where $\rho(r, t)$ is the number density of the GCS, $v_r(r, t)$ is its radial velocity field and $S \geq 0$ is a ‘sink’ term. We have written the continuity equation in spherical coordinates, dropping the terms containing the derivatives with respect to angles, since the observed GCSs usually show spherical symmetry. Moreover, we have adopted $v_\theta=0$ and $v_\phi=0$ since the GCSs seem not to rotate. If no evolution of the GCS occurs (as is the case when the system is collisionless and no massive central ‘absorber’ is present), we expect $v_r(r, t)=0$ and $S=0$ for any r and t . In our picture, instead, the frictional drag of the stellar halo on the GCS, reduces the energy of the clusters, acting as a radial velocity field pointing inward. At the same time, the massive galactic nucleus erodes the GCS, standing for a non-zero sink term $S = \rho/\tau_{tid}$, where, hereafter, τ_{tid} , is the average of formula (2) over the DF of the system, as described in Appendix A. Once we give the initial GCS density distribution $\rho(r, 0)$, and we assume $v_r(r, t)=v_r(r)$ (that is, the radial velocity field generated by the unevolving stellar halo does not change during the evolution of the system), the following solution of Eq. (3) is obtained (see Appendix B):

$$\begin{aligned} \rho(r, t) &= \frac{v_r(H(r, t))H^2(r, t)}{v_r(r)r^2} \rho(H(r, t), 0) \times \\ &\times \exp\left(-\int_0^t \frac{dx}{\tau_{tid}(H(r, x), M_n(t-x), \bar{\rho}_h)}\right) \end{aligned} \quad (4)$$

where

$$H(r, t) = H(t + \tau(r)) \quad (5)$$

$$\tau(r) = -\int \frac{dr}{v_r(r)} \quad (6)$$

and $H(x)$ is the inverse function of $\tau(r)$. The function $M_n(t)$, which gives the nucleus mass at any time t , is not known. In our calculations, we will adopt a fixed nucleus mass since a reliable evaluation of the rate of accretion of the nucleus requires further investigation (see Capuzzo-Dolcetta 1996). Anyway, when a realistic model will be available to give $M_n(t)$, it will be straightforwardly included in our model.

By the definition of $\tau(r)$, the difference $\tau(R) - \tau(0)$ is the time required to an element of mass of the ‘fluid’ to reach the centre and stop there, starting from a point at distance R from the origin. It is so straightforward to relate this $\tau(r)$ to the function $\tau_{df}(E, m)$. This is easily done by averaging $\tau_{df}(E, m)$ over the DF of the system, thus obtaining a function $\tau_{df}(r, m)$ (see Appendix B). Now, the velocity field at any point r can be estimated by

$$v_r(r, m) = -\frac{r}{\tau_{df}} \quad (7)$$

Thus, substituting Eq. (7) in Eq. (6), we find the following expression for the function $\tau(r)$ which appears in the solution (4):

$$\tau(r, m) = \int \frac{\tau_{df}}{r} dr. \quad (8)$$

In this way we have related the dynamical friction effect to the presence of a velocity field pointing radially inward. As expected, $\rho(r, t)$ as given by Eq. (4), depends on m via Eq. (8). In the following, we assume the initial distribution of the GCS in the form

$$\rho(r, 0; m) = \psi_0(m) \cdot \rho(r, 0) \quad (9)$$

where m is the individual cluster mass and $\psi_0(m)$ is the GCS’s initial mass function (hereafter IMF). The relation (9) says that the IMF of the GCS is independent of the position in the system. The solution of eq. (3), in this case, is given by a superposition of distributions:

$$\rho(r, t) = \int_{m_1}^{m_2} \rho(r, t; m) \psi(m) dm \quad (10)$$

where $\rho(r, t; m)$ is the solution (4) for a single mass GCS, taking into account the dependence of τ_{df} on the clusters’ mass, m . To conclude, the dependence on the overall model is given by the functions τ_{df} and τ_{tid} , and by the GCS’s DF which fixes its initial distribution. It is clear, hence, that equations (4) and (10) may represent the evolution of a GCS in different situations, provided we know τ_{df} , τ_{tid} and $f(E)$.

3 THE RESULTS

In the previous Section we have solved the evolution equation for the density distribution of a GCS made up of clusters of different masses when dynamical friction and tidal disruption are taken into account. Before showing the results, we specify the parameters which our model depends on.

For $\bar{\rho}_h$, we seek a relation with the cluster mass. From data of clusters in our Galaxy (Webbink 1985) we found a loose relation among the mass and the half-mass density of the clusters, obtained by adopting a fixed ratio $(M/L_V)_\odot=1.5$ and fitting the clusters density profiles with Plummer models:

$$\bar{\rho}_h = 1.38 \cdot 10^5 m^{1.56} M_\odot pc^{-3} \quad (11)$$

This choice for the cluster half-mass density is quite different from that used by OBS in their calculations. Their GCS is composed of identical clusters with half-mass density $\bar{\rho}_h = 10^3 M_\odot pc^{-3}$, implying that we are dealing with clusters significantly denser than theirs. Since the tidal disruption timescale depends on $\sqrt{\bar{\rho}_h}$, we expect a lesser depletion of the GCS.

As initial single-mass number density for the GCS we assume:

$$\rho(r, 0) = \frac{\rho_0}{\left[1 + \left(\frac{r}{r_{c0}}\right)^2\right]^{\frac{3}{2}}} \quad (12)$$

which corresponds to the monopole component of the Schwarzschild potential, ρ_0 being the central density and r_{c0} the initial core radius (assumed equal to the bulge star core. Note that the projection, $\Sigma(r)$, of (12) is the so-called modified Hubble law, a function well fitting the elliptical galaxies’ surface brightness:

$$\Sigma(r, 0) = \frac{\Sigma_0}{1 + \left(\frac{r}{r_{c0}}\right)^2} \quad (13)$$

where $\Sigma_0 = 2\rho_0 r_{c0}$. Since the density distribution (12) has an infinite mass we cut it at a radius $r_{max} \gg r_{c0}$. Varying the value of r_{max} results in a different behaviour of the averaged timescales τ_{df} and τ_{tid} . Anyway, we find that, letting r_{max} to vary in a reasonable range, the differences are more important in the outer regions ($r \geq 20 r_{c0}$), where, anyway, the timescales are always sensibly longer than a Hubble time.

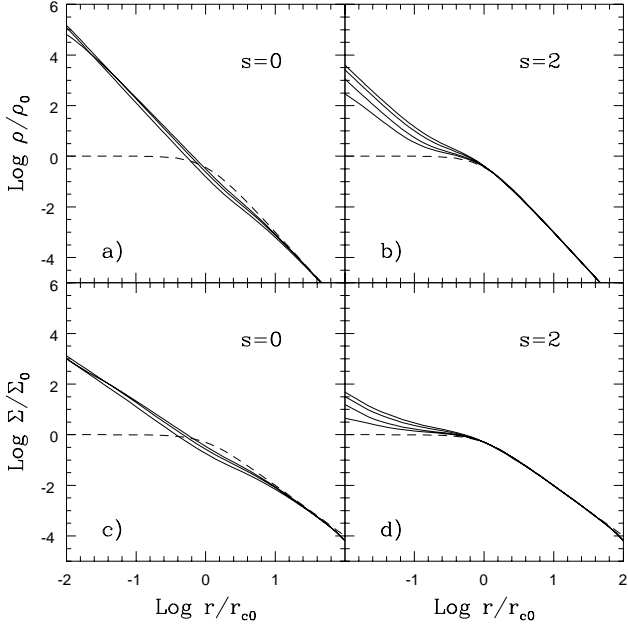


Figure 1. Evolution of the GCS space and surface density (upper and lower panels, respectively) due to dynamical friction only. Left panels: flat ($s=0$) IMF; right panels: steep ($s=2$) IMF. The thick curve is the initial distribution, the other curves correspond to 1, 5, 10 and 15 Gyr (bottom to top)

In the regions of interest ($r \leq 10 r_{c0}$), the changes in r_{max} reflect in negligible changes in our timescales.

As DF for the GCS, we use a King model with $\sigma^2 = 8\Phi_0$ (see eq. 4-130 and 4-131 in BT), whose corresponding density profile fits well eq. (12), as required.

For the GCS IMF we shall assume truncated power-laws:

$$\psi_0(m) = \begin{cases} 0 & 0 < m < m_1 \\ k m^{-s} & m_1 \leq m \leq m_2 \\ 0 & m > m_2 \end{cases} \quad (14)$$

with $m_1 = 10^4 M_\odot$ and $m_2 = 3 \cdot 10^6 M_\odot$, so that the product $\psi_0(m)\rho(r, 0)$ gives the initial number per unit volume of clusters with mass m . We consider the two cases of a flat ($s=0$) and a steeply decreasing ($s=2$) IMF. The normalization factor $k\rho_0$ is chosen in such a way to give a total number of clusters $N_{tot}=1000$.

3.1 Dynamical friction

When a pre-existing nucleus is absent - or its mass is so small that the tidal disruption effect is negligible - we may apply formula (B.11) for the evolution of the number density distribution of a GCS undergoing dynamical friction only. The results are shown in Fig. 1. We observe an inner region (within $r \approx r_{c0}$) where the density is strongly enhanced, surrounded by a depleted strip ($r_{c0} \leq r \leq 10 r_{c0}$). This effect is best seen in the $s=0$ case (Fig. 1a,c), since, with such an IMF, the GCS is composed by a large fraction of massive clusters, which decay faster. On the contrary, with a steep ($s=2$) IMF (Fig. 1b,d), the GCS is composed mainly of light clusters, which respond slowly to the frictional drag,

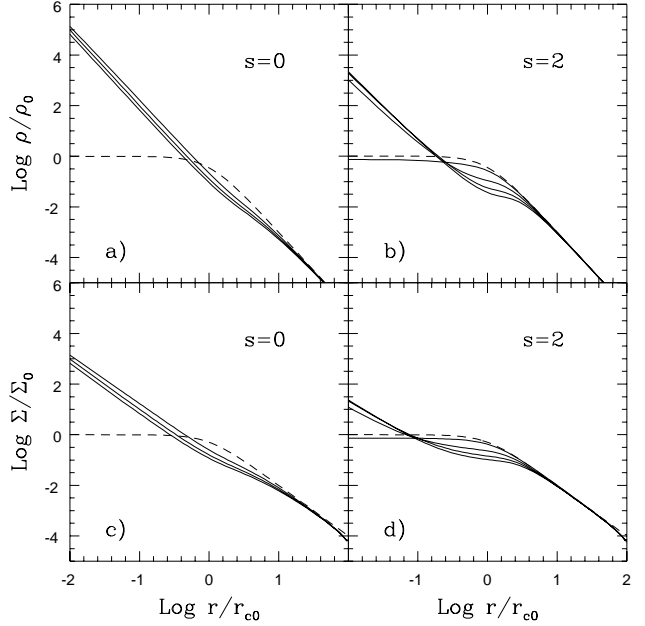


Figure 2. Same as Fig.1, taking into account tidal disruption of clusters by a nucleus of fixed mass $M_n=10^7 M_\odot$. The thick curve is the initial distribution, the curve corresponding to 1 Gyr is the closest in shape to the initial distribution and the other curves correspond to 5, 10 and 15 Gyr (top to bottom)

thus the depletion in the outer region is almost imperceptible. The surface distributions, in both cases, become more concentrated as time goes on, so that the core radii become smaller. This is a natural consequence of the fact that globular clusters lose their energy by dynamical friction and move on less extended orbits.

To study the time evolution of the core radius of the GCS, we need to remember that an actual observation cannot sample the GCS distribution all the way to the centre of the galaxy. As a consequence, the value of the observed core radius depends on a somewhat arbitrary extension of the GCS' surface density towards the centre of the galaxy. Were the inner limit of the observations equal to, say, r_{c0} , in the $s=2$ case we would not observe any differences between the halo and GCS distributions (Fig. 1d); in the $s=0$ case we would observe a flatter slope (Fig. 1c), that would lead us to conclude erroneously that the GCS is less concentrated than the halo. Could we sample clusters to a smaller inner radius, say $0.1 r_{c0}$, we would observe that the GCS distributions, in both cases, are more concentrated than that of the halo. It is evident, then, the importance of going with the observations as close to the centre of the galaxy as possible. In the next Subsection we give a more detailed evaluation of the core radius of the evolved GCS.

It is interesting to calculate the number of clusters contained in a given radius R at time t , $N_{cl}(R, t)$. In the case of dynamical friction alone, the integral over r is easily done, and we obtain:

$$N_{cl}(R, t) = \int_{m_1}^{m_2} N_{cl}^0(H(t + \tau_{df}(R, m))) \psi_0(m) dm \quad (15)$$

where $N_{cl}^0(r)$ is the number of clusters in the sphere of radius

Table 1. Number and total mass of clusters inside one core radius at time 15 Gyr, compared to their initial values (with the subscript 0).

IMF	N_{cl0}	N_{cl}	M_{cl0} (M_{\odot})	M_{cl} (M_{\odot})
$s=0$	37	410	$5.6 \cdot 10^7$	$7.2 \cdot 10^8$
$s=2$	37	66	$2.1 \cdot 10^6$	$1.2 \cdot 10^7$

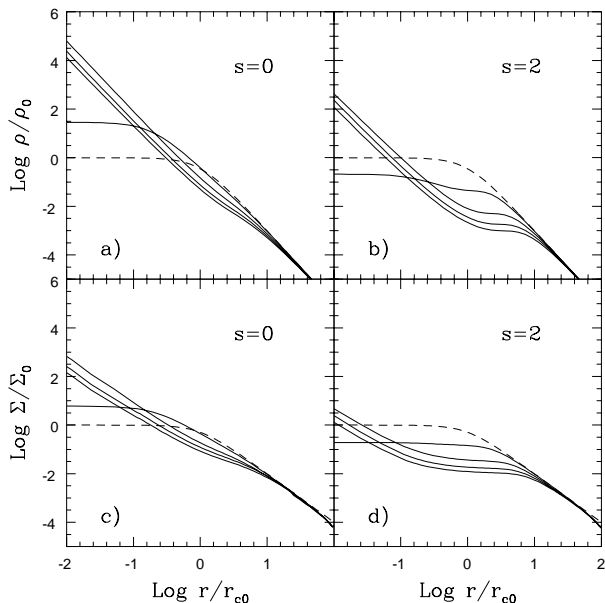


Figure 3. Same as Fig.2, but $M_n=10^8 M_{\odot}$.

r at $t = 0$. A similar equation holds for the mass contained in the sphere of radius R at time t , $M_{cl}(R, t)$. In this way, we can evaluate the number and mass of clusters within the core at present time ($t=15$ Gyr), N_{cl} and M_{cl} , and compare them with their initial values, N_{cl0} and M_{cl0} (see Table 1). This table gives a first insight on the possible formation of a massive nucleus by globular clusters accretion, since the M_{cl} values constitute the upper limits to the mass contribution by the cluster system. It is easily seen that $N_{cl}(R, t)$, as well as $M_{cl}(R, t)$, scale linearly with N_{tot} . So, bigger values for the mass inside the core radius require larger N_{tot} , which is not a free parameter, being constrained by observations, through the presently observed number of clusters.

3.2 Dynamical friction and tidal disruption

Now, we show the results for the volume density and surface distribution of a GCS subjected to both dynamical friction and tidal disruption. As it is easily seen, in Figs. 2, 3 and 4 the density profiles strongly depend on M_n .

The role of the nucleus is overwhelming when the GCS is composed mainly of low-density clusters ($s=2$ case, see Eq. (11)). In this case, the profiles differ significantly from the case of the absence of a nucleus, even if the nucleus mass is moderate ($M_n=10^7 M_{\odot}$, compare Fig. 1b,d to 2b,d). On the contrary, the more massive clusters of the flat IMF, being denser, resist effectively to the tidal disruption when $M_n \leq 10^7 M_{\odot}$ (compare Fig. 1a,c to 2a,c). Of course the de-

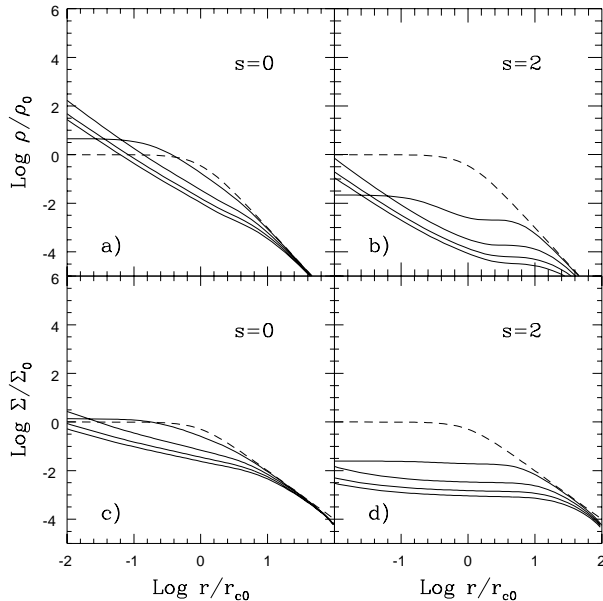


Figure 4. Same as Fig.2, but $M_n=10^9 M_{\odot}$.

pauperating effect of tidal disruption is enhanced by heavier nucleus masses (see Fig. 3 and 4).

Another interesting feature is the prominent central density cusp, more evident for light nuclei and flat IMF. This is due essentially to heavy clusters which rapidly move towards the centre of the galaxy due to large dynamical friction suffered by their high mass, and contemporarily survive tidal disruption because of their high density. At increasing nucleus masses, this effect is less evident and becomes almost imperceptible for heavy nuclei, because of the increasing efficiency of tidal disruption. Note how the differences among the density profiles of the innermost and external regions are significantly reduced by projection (compare upper and lower panels in Fig. 2,3 and 4).

3.2.1 The GCS core radius evolution

In the $s=2$ case for the IMF, the surface distributions depart from a modified Hubble law just in the inner regions, thus leading to a reliable r_c determination. With a flat IMF, instead, no region of constant density (a ‘core’) is kept up to present time. Anyway, observationally, the steepening of the profile (which carries the signature of dynamical friction) could be appreciated just inside a region whose radius is of the order of r_{c0} . In this case, the evaluation of r_c depends on the extension of the observed profile towards the centre, which usually results in its overestimate. To give a quantitative evaluation of this overestimate, we have calculated the ‘observable’ core radii of the GCS after a dynamical evolution of 15 Gyr, by fitting the surface density profiles of Fig. 5 with modified Hubble laws. By ‘observable’ we mean that the fits were done excluding too inner regions, within some radius r_{min} . The results are given in Tables 2 and 3, for different nucleus masses. In the $s=2$ case the value of r_c does not change much on varying r_{min} , confirming that the surface distribution of the GCS is well approximated by a

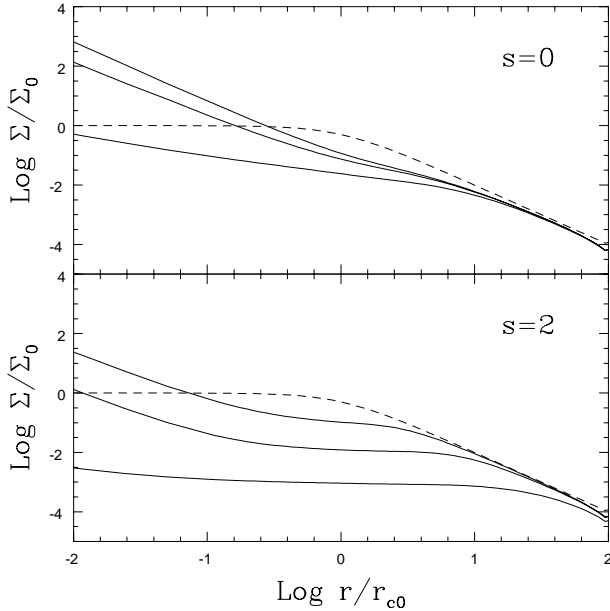


Figure 5. Plot of the GCS surface density profile after evolution has occurred for a flat ($s=0$) IMF (upper panel) and for a steep ($s=2$) IMF (lower panel). The thick curve is the initial profile, the other curves correspond to nucleus masses of 10^7 , 10^8 and $10^9 M_{\odot}$ (top to bottom).

Table 2. ‘Observed’ core radius for the case of a flat IMF ($s=0$).

r_{min}	$M_n=10^7$	$M_n=10^8$	$M_n=10^9$
$r_{c0}/2$	2.7	8.7	24.0
r_{c0}	3.0	9.3	25.0
$5 r_{c0}$	3.0	9.3	25.0

Values obtained by fitting the surface density profiles of the evolved GCS with a modified Hubble law, excluding the region inside r_{min} , for different nucleus masses M_n .

modified Hubble law. On the contrary, in the $s=0$ case, the observed core radius depends strongly on the value of r_{min} , indicating that the surface distribution does not display a well defined central core. Then, a core is reliably defined when clusters have been destroyed by tidal disruption.

In Fig. 6, we plot, for the steep IMF, the time evolution of the ‘observed’ core radius for different nucleus masses, obtained as described above.

3.2.2 A parameter reliably comparable with observations

A better parameter to synthesize the properties of the evolved GCSs is given by $x = N_l/N_0$, defined as the ratio between the number of ‘lost’ clusters outside the min-

Table 3. Same as Table 2, but for the case of a steep IMF ($s=2$).

r_{min}	$M_n=10^7$	$M_n=10^8$	$M_n=10^9$
$r_{c0}/2$	0.8	0.8	1.6
r_{c0}	1.4	2.0	4.2
$5 r_{c0}$	4.6	5.2	7.5

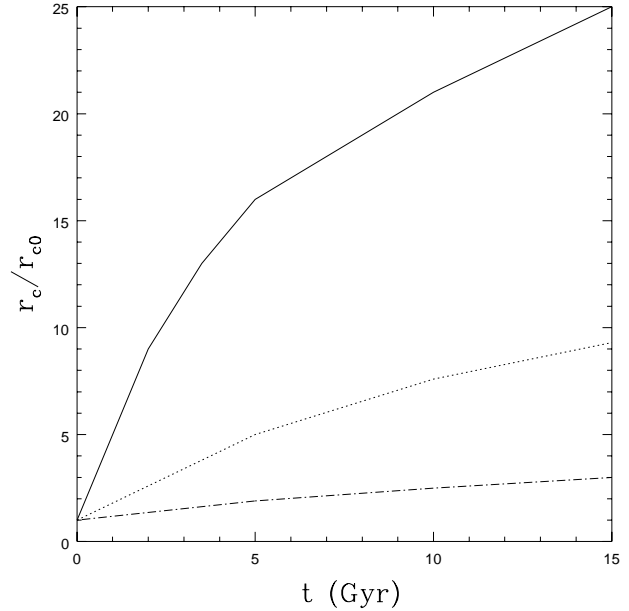


Figure 6. Time evolution of the ‘observed’ core radius for a GCS with a steep ($s=2$) IMF and $M_n=10^7 M_{\odot}$ (dot-dashed curve), $M_n=10^8 M_{\odot}$ (dotted curve), $M_n=10^9 M_{\odot}$ (solid curve)

Table 4. Fraction of ‘lost’ clusters after 15 Gyr.

$M_n (M_{\odot})$	$s=0$	$s=2$
10^7	0.40	0.20
10^8	0.42	0.46
10^9	0.51	0.78

imum radius reachable by the observations (r_{min}) to the initial number of clusters in that region. The number N_l is given by the difference between the initial and the present number of clusters, outside r_{min} . The ‘lost’ clusters include either clusters which have been actually destroyed by tidal interaction with the massive nucleus either clusters which have lost energy by dynamical friction and have moved on orbits all within r_{min} .

The quantity x is a good parameter to quantify the roles of the evolutionary mechanism under discussion, because it could be easily inferred from observations, as the difference observed between the (normalized) radial profiles of halo stars and GCS. This requires the reasonable hypothesis that the initial distributions of clusters and bulge stars were the same and that the present bulge distribution is equal to the initial (see McLaughlin 1995, Capuzzo-Dolcetta & Vignola 1996). In Table 4 we give the fraction of ‘lost’ clusters for a GCS subjected to dynamical friction and tidal disruption with different nucleus masses and for the two IMFs, with $r_{min} = r_{c0}$. For the flat IMF, x varies of just 25 per cent at varying the nucleus mass from $10^7 M_{\odot}$ to $10^9 M_{\odot}$, indicating that dynamical friction is important. For the less dense clusters of the steep IMF x increases by a factor four over the same M_n range because, in this case, tidal disruption is dominant.

To understand better the contributions of the two depleting mechanisms and their dependence upon the relevant

parameters (nucleus mass and clusters' half mass density) we have followed the evolution of the GCS density profiles in two limiting cases: *i*) pure dynamical friction and *ii*) pure tidal disruption. The computations were performed on various single-mass GCSs, over a range of individual cluster masses m , choosing $r_{min} = r_{c0}$.

In case *i*), the results at time 15 Gyr are well fitted by a broken power-law,

$$x_{df} = \begin{cases} 0.46 \cdot m^{0.82} & 0.01 \leq m \leq 0.6 \\ 0.35 \cdot m^{0.36} & 0.6 < m < 3 \end{cases} \quad (16)$$

where m is in $10^6 M_{\odot}$. For a GCS with a distribution of masses it is quite natural to calculate the quantity x_{df} by averaging it on the IMF. This leads to an error of about 3 per cent respect to the exact result obtained by integrating the volume density given by Eq. (10), indicating as reliable the simple average of the expression (16) on different IMFs. For our models, we obtain: for a flat IMF, $x_{df}=0.38$; for a steep IMF, $x_{df}=0.04$. Clearly the influence of dynamical friction is almost negligible if the GCS's initial mass function is biased towards light clusters.

In case *ii*), we expect that x_{tid} depends on the nucleus mass and cluster half-mass density through the combination $M_n/\sqrt{\rho_h}$. In fact, we find that a good fit to x_{tid} is

$$x_{tid} = \begin{cases} 6.79 \cdot 10^{-5} y^{0.79} & 0 \leq y \leq 7.47 \cdot 10^5 \\ 0.17 \cdot y^{0.21} & y > 7.47 \cdot 10^5 \end{cases} \quad (17)$$

where $y = M_n \cdot \bar{\rho}_h^{-1/2}$, $\bar{\rho}_h$ is in units of $M_{\odot} \cdot \text{pc}^{-3}$ and M_n in solar masses. Like before, to obtain the quantity x_{tid} for a GCS with a distribution of masses we average the expression (17) on the IMF.

When both the effects are at work, a reasonable expression for x would be, clearly:

$$x = x_{df} + (1 - x_{df}) x_{tid}. \quad (18)$$

The values obtained in this way are in good agreement with the $s=2$ case of Table 4, since $x_{df} \ll x_{tid}$, while the $s=0$ case is poorly represented because the two effects compete.

3.3 The evolution of the mass function

Since both dynamical friction and tidal disruption timescales depend differently on the cluster mass, the IMF given by Eq. (13) evolves into a mass function which is different from point to point in the system.

In Fig. 7 we show the present time mass function of the GCS for different nucleus masses (excluding the region within r_{c0} to make it comparable to radially limited observed samples).

Note that, as long as the GCS mass contribution to the nucleus is negligible, the knowledge of the evolution of a particular mass function allows to obtain the evolution of a different IMF. Indeed, under this hypothesis, the individual mass components of the GCS evolve independently of each other. Hence, the following relation among two mass functions ψ and ϕ

$$\frac{\psi_e}{\psi_0} = \frac{\phi_e}{\phi_0} \quad (19)$$

holds, where the subscript '0' stands for the IMF and the subscript 'e' stands for the evolved mass function. Thus,

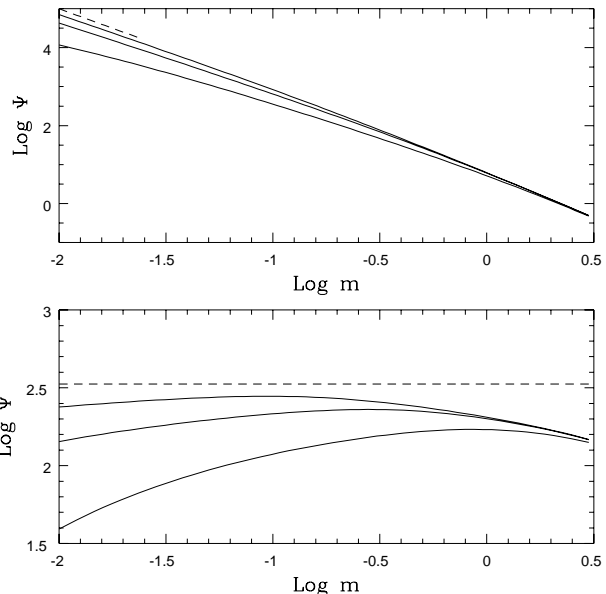


Figure 7. Evolved ($t=15$ Gyr) mass functions for different nucleus masses. Upper panel: steep ($s=2$) IMF; lower panel: flat ($s=0$) IMF. The thick solid curve is the IMF, the other curves correspond to $M_n=10^7$, 10^8 and $10^9 M_{\odot}$ (top to bottom). Cluster masses are in $10^6 M_{\odot}$; ψ in units such that $N_{tot}=1000$.

it is straightforward to obtain the initial mass function ϕ_0 from the evolved observed mass function ϕ_e via Eq. (19). Of course, some assumptions on the time evolution of the nucleus mass are needed. In a more detailed scenario, the GCS will contribute to M_n in a way dependent on the IMF, which means that Eq. (19) no longer applies.

4 CONCLUSIONS

In this paper we have developed a model which allows to follow the evolution of the density distribution of a globular cluster system (GCS) in a triaxial galaxy under the influence of two effects: dynamical friction by field stars and tidal disruption by a massive central object. Both these effects are amplified by the triaxiality of the gravitational potential of the parent galaxy. The exact knowledge of the present-time density profiles permits to calculate the value of some of the relevant observables as a function of the assumptions made on the initial distribution and mass function of the GCSs.

Actually, we find that the minor concentration of the GCSs, relatively to the distribution of halo stars, as observed in many galaxies, is an effect which depends strongly on the quality of the observations. In particular, a comparison of the core radius of the GCS with that (r_{c0}) of its parent galaxy star distribution might be misleading, since the estimate for the core radius of the GCS depends on the minimum radius at which clusters are sampled. For example, we have shown that, in the case of a GCS whose evolution is prevalently ruled by dynamical friction, as it is the case for a GCS made up mostly of heavy clusters, the final shape of the distribution displays a strong concentration of massive clusters in the very inner regions of the galaxy and a con-

sequent lack of clusters in the outer regions. In this case, if the observations do not reach the inner regions (within r_{c0}), we effectively measure an erroneously large core radius. Thus, an observed larger core radius is not a firm signature of the presence of a massive object at the centre of the galaxy. However, we found noticeable differences among the case of a steep IMF and that of a flat IMF. These differences, due to the influence of the half-mass density of the clusters as a function of the cluster mass, are such that:

i) for a steep IMF, made up mostly of light clusters, the prevailing effect is tidal disruption and there is a strong dependence of the evolved core radius on the mass of the central object (the value $r_c = 10r_{c0}$ is obtained with a nucleus of $2 \cdot 10^8 M_\odot$);

ii) for a flat IMF, made up mostly of heavy (and dense) clusters, the prevailing cause of depletion is dynamical friction and, consequently, the dependence on the mass of the central object is weak ($r_c = 10r_{c0}$ for $2 \cdot 10^9 M_\odot$).

We have found that a parameter which is more reliable than the core radius to describe the GCS is the number of ‘lost’ clusters outside some minimum radius (we choose $r_{min} = r_{c0}$). This is the difference between the initial and the observed number of clusters, under the assumption that the GCS was initially distributed as the parent halo light. Our calculations show that: for a flat IMF the percentage of ‘lost’ clusters ranges from 40 per cent (with no massive central object) to 50 per cent (for a $10^9 M_\odot$ nucleus) of the initial total number; for a steep IMF it ranges from 3 per cent (no nucleus) to 80 per cent ($10^9 M_\odot$ nucleus).

We give two formulas which fit the fraction of ‘lost’ clusters in the case of dynamical friction only and in the case of tidal disruption only, as a function of the cluster mass. When both the effects are working, the number of ‘lost’ clusters may not be obtained by simply summing the fractions, confirming that an interaction among the two effects exists.

To conclude, our calculations show that the present differences observed between the GCS and halo stars surface distributions *can be explained by dynamical evolution of the GCS, under the influence of dynamical friction and tidal disruption*, even if the initial concentrations (core radii) were the same. Thus, to have a definite answer to the question “are the observed differences between the star-bulge and the GCS density profiles just reflecting different initial conditions or are a consequence of evolution?”, it would be crucial to compare their kinematical properties. For example, the knowledge of the run with radius of the GCS (projected) velocity dispersion may help to understand if, like in our galaxy, there has been a selective depauperation of clusters on highly radial orbits.

REFERENCES

- Bertola, F., Vietri, M. & Zeilinger, W.W. 1991, ApJL, 374, L13
 Binney, J.J., 1988. in: Cooling Flows, p.225, ed. Fabian A., Reidel, Dordrecht.
 Binney, J.J. & Tremaine, S.D., 1987. Galactic Dynamics, Princeton University Press, Princeton.
 Capuzzo-Dolcetta, R. 1993, ApJ, 415, 616
 Capuzzo-Dolcetta, R. 1997, in preparation
 Capuzzo-Dolcetta, R. & Vignola, L. 1996, submitted to A&A
 Dressler, A. & Richstone, D. O. 1988, ApJ, 324, 701
 Eckart, A. & Genzel, R. 1996, Nature, 383:415

- Forbes, D. A., Franx, M., Illingworth, G. D., Carollo, C. M. 1996, ApJ, 467, 126
 Frenk, C. & White, S.D.M., 1980, MNRAS, 193, 295
 Freeman, K.C. 1993, in The Globular Cluster-Galaxy Connection, ASP Conference Series, vol. 48, ed. G.H. Smith & J.P. Brodie, p.27
 Harris, W.E. 1986, AJ, 91, 822
 Harris, W.E. 1991, ARA&A, 29, 543
 Harris, W.E. & Racine, R. 1979, ARA&A, 17, 241
 Kormendy, J. 1988, ApJ, 325, 128
 Kormendy, J. & Richstone, D. 1995, ARA&A, 33, 581
 Lauer, T. R. & Kormendy, J. 1986, ApJL, 303, L1
 Mayoz E., 1995, ApJL, 447, L91
 Miyoshi, M., Moran, J., Herrnstein, J., Greenhill, L., Nakai, N. et al. 1995, Nature, 373:127
 Ostriker, J.P., Binney, J. & Saha, P. 1989, MNRAS, 241, 849
 Pesce, E., Capuzzo-Dolcetta, R. & Vietri, M. 1992, MNRAS, 254, 466
 Plummer, H. C. 1911, MNRAS, 71, 460
 Racine, R. 1991, AJ, 101, 865
 Schwarzschild, M. 1979, ApJ, 232, 836
 Tremaine, S.D., Ostriker, J.P. & Spitzer, L. 1975, 196, 407
 van Albada, T.S., 1982, MNRAS, 201, 939
 Webbink, R. F. 1985, IAU Simp. 113, Dynamics of Star Clusters, ed. J. Goodman & P. Hut (Dordrecht: Reidel), 541

APPENDIX A:

The relation

$$r_a = u^{-1}(E) \quad (\text{A1})$$

holds between the orbital energy E and apocentric distance r_a , where $u(r)$ is the spherical symmetric component of the Schwarzschild’s potential (see Eq. (5) in Pesce et al. 1992). Eq. (A1) suffices to give τ_{tid} as a function of E . At any point r , we average the tidal disruption timescale on the distribution function, $f(E)$, of the clusters system, thus obtaining an averaged tidal disruption timescale:

$$\begin{aligned} \tau_{tid}(r; M_n, \bar{\rho}_h) &= \langle \tau_{tid}(E, M_n, \bar{\rho}_h) \rangle_{DF} = \\ &= \frac{\int \tau_{tid}(E, M_n, \bar{\rho}_h) \cdot f(E) v^2 dv}{\int f(E) v^2 dv} \end{aligned} \quad (\text{A2})$$

where the integration is done on the region of phase-space corresponding to bound orbits. In the same way, we may obtain an averaged dynamical friction timescale

$$\begin{aligned} \tau_{df}(r, m) &= \langle \tau_{df}(E) \rangle_{DF} = \\ &= \frac{\int \tau_{df}(E) \cdot f(E) v^2 dv}{\int f(E) v^2 dv} \end{aligned} \quad (\text{A3})$$

APPENDIX B:

First of all, we seek a solution, say $\bar{\rho}$ of the continuity equation in its homogeneous form, that is:

$$\frac{\partial \rho}{\partial t} + \frac{\partial \rho v_r}{\partial r} + 2 \frac{\rho v_r}{r} = 0 \quad (\text{B1})$$

An exact analytical solution is easily found when $v_r(r, t) = u(r)w(t)$, in the following way.

We define the quantity $N(r, t)$ as

$$N(r, t) = 4\pi \int_0^r \rho(r', t) r'^2 dr' \quad (\text{B2})$$

Now, integrating Eq. (B1) over the same spherical volume as in Eq. (B2), we obtain an equation for $N(r, t)$:

$$\frac{\partial N}{\partial t} + v_r \frac{\partial N}{\partial r} = 0. \quad (\text{B3})$$

If we define the functions

$$\tau(r) = - \int \frac{dr}{u(r)} \quad (\text{B4})$$

and

$$W(t) = \int \frac{dt}{w(t)}, \quad (\text{B5})$$

Eq. (B3) becomes

$$\frac{\partial N}{\partial W} - \frac{\partial N}{\partial \tau} = 0. \quad (\text{B6})$$

whose solution is:

$$N(r, t) = F(W(t) + \tau(r)) \quad (\text{B7})$$

where $F(x)$ is a function constrained by the initial conditions on $\rho(r, t)$. The solution $\tilde{\rho}(r, t)$ is obtained by inverting Eq. (B2):

$$\tilde{\rho}(r, t) = \frac{1}{4\pi r^2} \cdot \frac{\partial N}{\partial r} = \frac{1}{u(r)r^2} f(W(t) + \tau(r)) \quad (\text{B8})$$

Assuming an initial density distribution $\tilde{\rho}(r, 0)$, we find the relation

$$f(x) = \tilde{\rho}(H(x), 0) u(H(x)) H(x)^2 \quad (\text{B9})$$

where $H(x) \equiv \tau^{-1}(x)$. Finally, the solution of the homogeneous continuity equation is

$$\begin{aligned} \tilde{\rho}(r, t) &= \frac{u(H(W(t)+\tau(r)))H^2(W(t)+\tau(r))}{u(r)r^2} \times \\ &\times \tilde{\rho}(H(W(t) + \tau(r)), 0) \end{aligned} \quad (\text{B10})$$

For the purposes of this paper, we set $w(t)=1$ (see Sect. 2), so that $W(t)=t$ and the solution (B10) simplifies to:

$$\begin{aligned} \tilde{\rho}(r, t) &= \frac{u(H(t+\tau(r)))H^2(t+\tau(r))}{u(r)r^2} \times \\ &\times \tilde{\rho}(H(t + \tau(r)), 0) \end{aligned} \quad (\text{B11})$$

When a ‘sink’ term, $S(r, t)$, is present (see Eq. (3)), the solution is in the form

$$\rho(r, t) = \tilde{\rho}(r, t) \cdot E(r, t) \quad (\text{B12})$$

where $E(r, t)$ satisfies

$$\frac{\partial \ln E}{\partial t} + v_r \frac{\partial \ln E}{\partial r} + S(r, t) = 0 \quad (\text{B13})$$

The solution of (B13) is:

$$\ln E(r, t) = - \int_0^t S(H(x + \tau(r)), t - x) dx. \quad (\text{B14})$$

Thus, the solution when a sink term is present specifies to:

$$\rho(r, t) = \rho_{om}(r, t) \cdot e^{-\int_0^t S(H(x+\tau(r)), t-x) dx} \quad (\text{B15})$$

This paper has been produced using the Royal Astronomical Society/Blackwell Science L^AT_EX style file.